Activation of soil and chemical reagents exposed to the neutrons released by the JCO criticality accident in Tokai-mura.

J. RADIAT. RES., 42: SUPPL., S55–S74 (2001)

Activation of Soil and Chemical Reagents Exposed to the Neutrons Released by the JCO Criticality Accident in Tokai-mura

YOSHIMASA MURATA[1]*, TOSHIHARU MUROYAMA[1], YOSHIKO KAWABATA[1], MASAYOSHI YAMAMOTO[1] and KAZUHISA KOMURA[1]

[1]Low Level Radioactivity Laboratory, Kanazawa University, Wake, Tatsunokuchi, Ishikawa 923–1224, Japan

JCO criticality accident/Neutron activation/Neutron fluence/Soil/Chemical reagent

Specific activities (Bq/g-element) of residual neutron-induced radionuclides by the JCO criticality accident were measured for soil, concrete block and chemical reagent samples collected in the JCO campus. Induced radionuclides such as ^{24}Na, ^{46}Sc, ^{54}Mn, ^{59}Fe, ^{60}Co, ^{65}Zn, ^{82}Br, ^{122}Sb, ^{134}Cs and ^{140}La were detected in the samples, depending on the ground distance from the accident point and the sampling date. Apparent thermal, epi-thermal and fast neutron fluences, which reached the sample at each point, were roughly estimated from the specific activities and cross sections of the target nuclides taken from a literature. The present data are believed to be important as validation data for a three-dimensional neutron transport model calculation.

INTRODUCTION

On September 30 1999, a criticality accident occurred at the uranium conversion building in the JCO campus, Tokai-mura, Japan. The distinct feature of this accident was the continuous release (about 20 hours) of fission neutrons to the environment without an appreciable release of fission products. To evaluate the neutron doses to residents living near the JCO campus and environmental effects, a research group was organized (leader: Prof. K. Komura, Kanazawa University). Six campaigns to the accident site and its vicinity were conducted to collect samples. The preliminary results obtained by this research group have already been published as a "Special Issue on the Tokai-mura Accident" in Journal of Environmental Radioactivity[1)]. In our previous work, only the concentrations (Bq/g-dry soil or g-reagent) of neutron-induced radionuclides in soil and chemical reagent samples were reported[2,3)]. Because their activity levels at the date of measurements were less than 1 Bq/g-dry soil for all radionuclides found, there is no need to worry about any harmful effect on the human body. Tentative estimates of the apparent thermal

*Corresponding author: Phone; +81–761–51–4440, Fax; +81–761–51–5528, E-mail; murata@llrl.ku-unet.ocn.ne.jp

and epi-thermal neutron fluences were made by using data obtained from chemical reagents[3].

In this paper, we present the specific activities found for all of the soil, concrete block and chemical reagent samples collected in the JCO campus. These results are expected to serve as basic data to estimate the neutron fluence and its energy spectrum. By using these data and the cross sections for well-moderated reactor neutrons[4], we tried to roughly estimate the thermal, epi-thermal and fast neutron fluences which reached samples. Furthermore, to serve as an aid to understand the activation of soil from the vicinity of the JCO criticality accident, neutron irradiation to soil samples were carried out using a research reactor. The results of this experiment were also compared with the data on residual neutron-induced radionuclides by the JCO criticality accident.

EXPERIMENTS

Sampling in the JCO campus

Soil samples were collected during the first and second surveys within the JCO campus (conducted on October 7 and 26, 1999). In the first sampling survey, surface soils of up to a depth of 5 cm were collected at 20 points by using a 5 cm cylindrical sampler. The second sampling

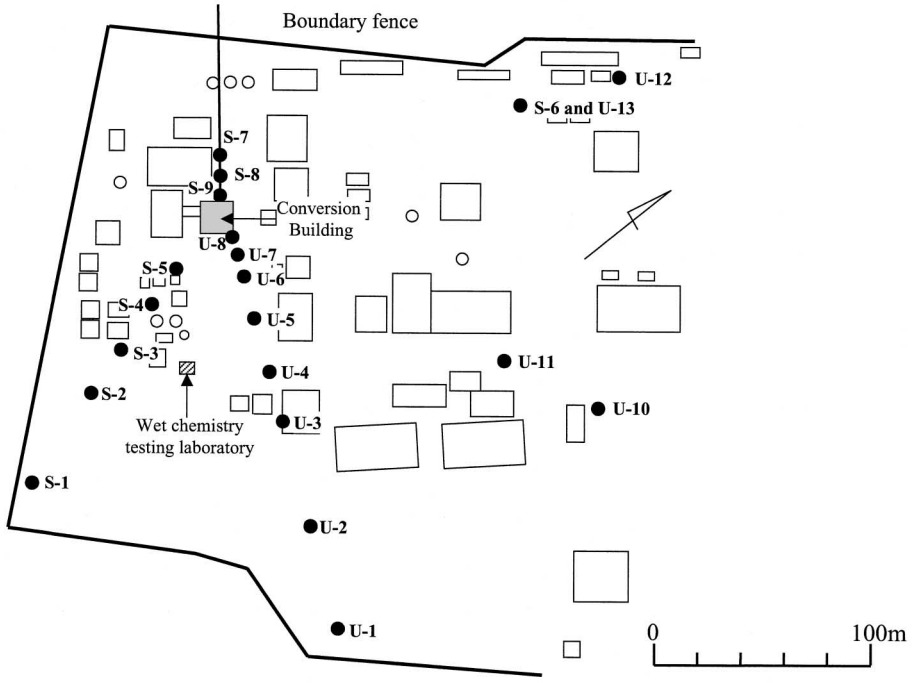

Fig. 1. Sampling points of soils in the first survey (October 7,1999). Chemical reagents were collected from the wet chemistry testing laboratory located about 65m SE of the conversion building in the second survey (October 26,1999).

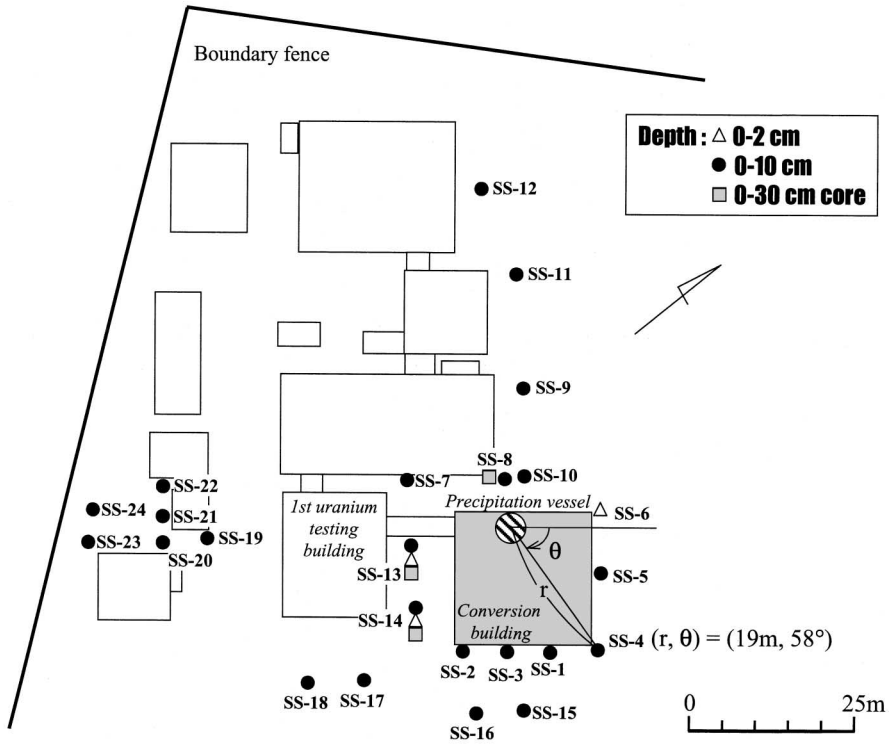

Fig. 2. Sampling points of soils in the second survey (October 26,1999).

was channeled towards an evaluation of the neutron fluence; at this time, surface (0–2 cm or 0–10 cm depth) and core (0–30 cm depth) soil samples were collected at 25 points by using mainly a 4.7 cm diameter sampler. The sampling points of soil in these surveys are shown in Figs. 1 and 2. In addition, a concrete block was collected in the fourth survey (November 27, 1999). This sample was collected at the ground surface just under the sampling point of a stainless-steel net cover of the water cooling tower of the air-conditioning equipment (only about 2.2 m from the precipitation vessel in which the criticality took place) reported by Nuclear Safety Commission[5]. Figure 3 shows the details of the sampling point of the concrete block.

Twenty chemical reagents were also collected on October 26, 1999, at the wet chemistry testing laboratory, located about 65 m SE of the precipitation vessel (Fig. 1). These chemical reagents, contained in 500g glass bottles and in smaller bottles or tubes, were placed on a reagent shelf at the corner nearest to the conversion building and upside or inside of the experimental table at the center of the room.

Measurements of radioactivities

The soil and reagent samples were brought back to the LLRL, then packed in a plastic case without any treatment, and measured for a half day to two days by Ge detectors to roughly estimate the radioactivity levels. Subsequently, the soil samples were air-dried, sieved through a 2

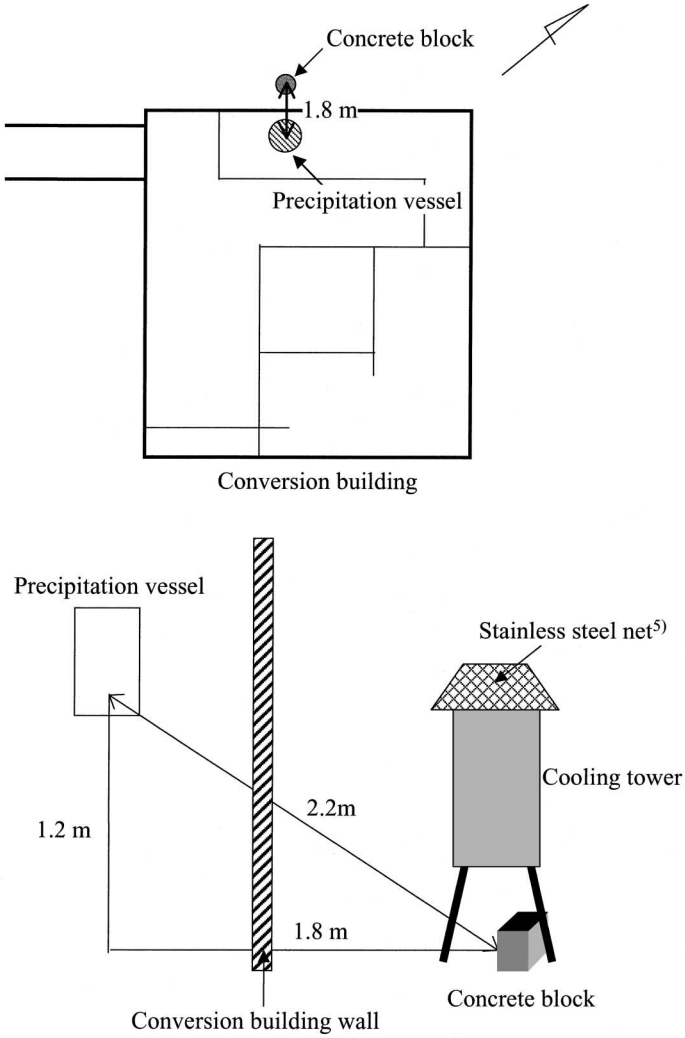

Fig. 3. Schematic view of the sampling point of a concrete block.

mm screen and homogenized in a mortar. The samples (50–80g) were packed into a plastic container with an inner diameter of 6 cm and a depth of 2 cm. The samples were then subjected again to a measurement for one to two days by the Ge detector. The concrete block was separated into several parts, as shown in Fig. 4. The samples were crushed into powder, packed in a plastic case and measured in a similar manner as mentioned above. The detectors used were calibrated with standards prepared from New Brunswick Laboratory (NBL) reference materials No.42-1 and analytical-grade KCl.

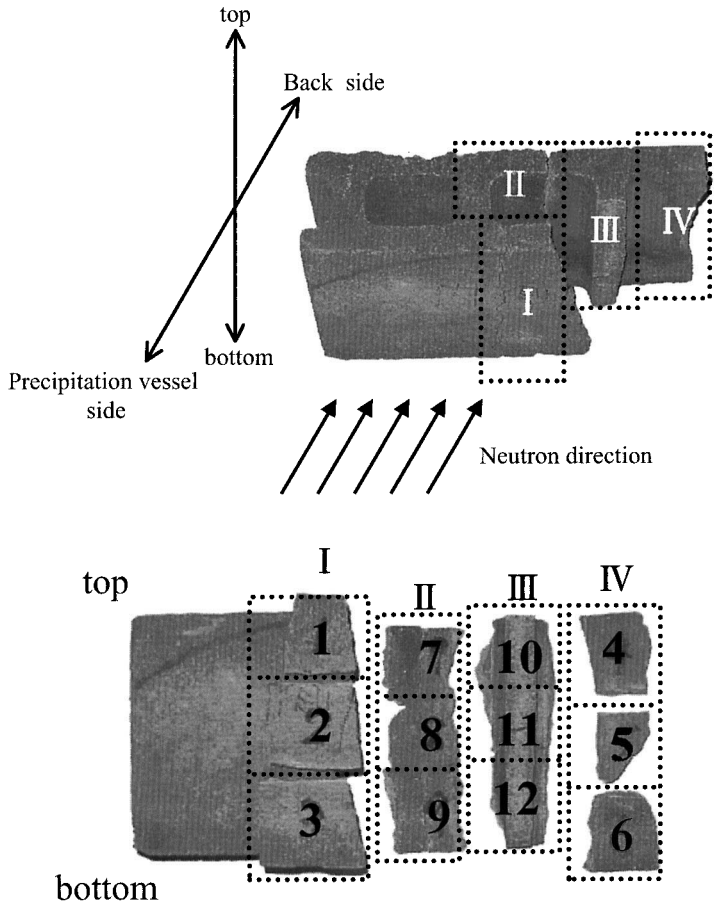

Fig. 4. Photograph of a concrete-block sample. Three and nine parts were separated from the facing part and back side of the concrete block, respectively.

Measurements of stable elements

The concentrations of Na, Sc, Fe, Co, Zn, Sb, Br, Cs and La in soil and concrete samples were determined together with the stable Co content in the Raney-Nickel reagent by NAA using the TRIGA Mark-II nuclear reactor at the Atomic Energy Research Institute of Rikkyo University. Aliquots (50–100 mg each) of dried samples were taken and heat-sealed in pre-cleaned polyethylene film. As reference samples, JB1 and JG1 issued by the Geological Survey of Japan, and some analytical grade reagents such as ZnO, Sb, CsCl were used.

Experiments of neutron-induced radionuclides in soil by research reactor

A known aliquot (7.48g, 15$\phi \times$ 19mm) of a soil sample (SS-8) collected in the JCO campus was irradiated by thermal neutrons at the University Training and Research Reactor of Kinki University (UTR-KINKI). The thermal output of this reactor is 1 W at full power operation and thermal neutron flux at central core position is evaluated to be 1×10^7 cm^{-2} s^{-1}. The total irradiated

Table 1. Specific activities in surface soil samples collected

Sampling points	Distance*	Direction*	Specific activities			
	r (m)	θ (°)	^{46}Sc/Sc	^{59}Fe/Fe	^{60}Co/Co	^{24}Na/Na
U-5	55	70	77 ± 9	0.023 ± 0.007		320 ± 110
U-6	35	65	190 ± 10	0.046 ± 0.006		250 ± 40
U-7	25	60	190 ± 10	0.066 ± 0.011		920 ± 50
U-8	16	90	320 ± 10	0.085 ± 0.008	19 ± 3	3300 ± 210
S-4	55	120	130 ± 20	0.039 ± 0.010		390 ± 60
S-5	35	120	60 ± 10			150 ± 30
S-7	25	280	120 ± 10	0.025 ± 0.006	11 ± 4	310 ± 80
S-8	15	285	730 ± 20	0.16 ± 0.01	36 ± 4	3160 ± 480
S-9	5	270	10600 ± 100	2.54 ± 0.03	500 ± 10	44000 ± 2100

* See Fig. 2

Table 2. Specific activities in surface soil samples collected

Sampling points	Distance*	Direction*	Specific activities		
	r (m)	θ (°)	^{46}Sc/Sc	^{59}Fe/Fe	^{60}Co/Co
SS-1	17	73	290 ± 20	0.055 ± 0.009	23 ± 5
SS-2	17	107	450 ± 20	0.12 ± 0.01	42 ± 7
SS-3	16	90	460 ± 20	0.11 ± 0.01	31 ± 5
SS-4	19	58	230 ± 20	0.077 ± 0.010	18 ± 6
SS-5	12	36	540 ± 20	0.14 ± 0.01	42 ± 5
SS-6	10	348	880 ± 40	0.23 ± 0.01	57 ± 8
SS-7	10	304	2420 ± 50	0.56 ± 0.02	122 ± 7
SS-8	6	239	3990 ± 70	1.01 ± 0.03	197 ± 10
SS-9	15	281	1920 ± 50	0.48 ± 0.02	121 ± 11
SS-10	6	301	5480 ± 10	1.49 ± 0.04	309 ± 14
SS-11	40	270	70 ± 10		
SS-12	52	265	37 ± 7		
SS-13**	11	153	2670 ± 60	0.72 ± 0.02	135 ± 10
SS-13	11	153	2150 ± 50	0.52 ± 0.02	117 ± 8
SS-14**	14	135	1230 ± 40	0.30 ± 0.02	76 ± 7
SS-14	14	135	1100 ± 30	0.27 ± 0.01	61 ± 5
SS-15	30	85	150 ± 10	0.025 ± 0.010	
SS-16	30	100	130 ± 10	0.026 ± 0.007	
SS-17	35	132	150 ± 10	0.19 ± 0.03	
SS-18	42	140	110 ± 10	0.067 ± 0.011	
SS-19	48	175	80 ± 20		
SS-20	55	175	50 ± 10		
SS-21	55	180	50 ± 10		
SS-22	55	185	26 ± 7		
SS-23	70	175	31 ± 8		
SS-24	70	180	38 ± 8		

* See Fig. 2

** These samples were collected by using a scoop

at the first JCO survey.

(Bq/g-element)					
^{140}La/La	^{134}Cs/Cs	^{65}Zn/Zn	^{122}Sb/Sb	^{82}Br/Br	^{54}Mn/Fe
770 ± 120					
1120 ± 110			6200 ± 600	710 ± 160	
620 ± 180					
2630 ± 510	60 ± 10		3900 ± 1800	1400 ± 200	
17200 ± 1300	550 ± 50	111 ± 8	19500 ± 6200	12600 ± 600	0.075 ± 0.005

at second JCO survey.

(Bq/g-element)			
^{134}Cs/Cs	^{65}Zn/Zn	^{124}Sb/Sb	^{54}Mn/Fe
		240 ± 180	
	12 ± 1		0.0073 ± 0.0018
290 ± 31	25 ± 3		0.028 ± 0.004
310 ± 41	34 ± 3		0.039 ± 0.005
256 ± 20	50 ± 2	3060 ± 40	
36100 ± 190	92 ± 6		
1440 ± 220	53 ± 5		
9260 ± 470	32 ± 3		
254 ± 145			

thermal neutron fluences were estimated to be 1.7×10^{11} cm^{-2}. Its fluence is nearly equal to the thermal neutron fluences in this sample from the JCO criticality accident. The soil sample exposed by reactor neutrons was brought back to the LLRL and a γ-ray measurement was conducted for one and half months.

RESULTS AND DISCUSSION

1. Specific activities of neutron-induced radionuclides

1.1 Surface soil

Neutron-induced radionuclides in surface soil samples are useful as an index in a quantitative evaluation of the spatial distribution of neutrons released at the criticality accident. Specific activities for radionuclides measured in the surface soil samples are summarized in Tables 1 and 2. All data, including Tables 5, 7 and 9 as shown hereafter, were decay-corrected to 6:14 a.m. on October 1, 1999, when the criticality ceased. As a result of the first survey (Table 1), 10 radionuclides were detected in the 9 samples within a 50 m circle from the center of the conversion building. ^{24}Na and ^{46}Sc were identified in the 9 samples, and ^{59}Fe, ^{60}Co, ^{65}Zn, ^{82}Br, ^{122}Sb, ^{134}Cs and ^{140}La were identified in a few samples. These nuclides seem to be produced mostly by thermal neutron capture reactions. The ^{54}Mn detected in sample S-9 is the only product by the fast neutron reaction ^{54}Fe(n, p)^{54}Mn. The specific activities for all radionuclides detected in the S-9 sample were the highest among the samples measured. This sample was collected at the nearest point, 5 m apart from the precipitation vessel. As for results of the second survey (Table 2), only 7 radionuclides were detected in the soil samples. Short-lived radionuclides such as ^{24}Na, ^{82}Br, ^{122}Sb and ^{140}La observed at the first survey could not be detected, because they had completely decayed out. ^{46}Sc was commonly observed for all of the samples, and ^{54}Mn, ^{59}Fe, ^{60}Co, ^{65}Zn, ^{124}Sb and ^{134}Cs were detected only for the samples collected near the conversion building.

The relationships between the specific activities and the slant distance from the precipitation vessel was then examined with the data classified by 8 directions. The results of ^{46}Sc, ^{59}Fe, ^{60}Co and ^{24}Na detected in many samples are shown in Fig. 5. The specific activity of each radionuclide decreases with increasing distance from the precipitation vessel. However, the directional dependence of the specific activity was not observed clearly for any radionuclides. Among these radionuclides, ^{46}Sc can be an index for the thermal neutron fluence. Because ^{45}Sc, which is a target nuclide of ^{46}Sc, has a two-times larger cross section for a thermal neutron than that for an epi-thermal neutron. The production of ^{46}Sc is, therefore, due mostly to the (n, γ) reaction by thermal neutrons. The directional independence of ^{46}Sc indicates that the angular spatial distribution of the thermal neutrons is independent on the direction. Takada et al.[6,7] reported a directional dependence by measuring β-rays in a concrete boundary wall of JCO. As for the directional dependence of released neutrons, a consideration of the fast neutrons is critical. We are now trying to measure ^{54}Mn formed by the ^{54}Fe(n, p)^{54}Mn reaction in soil samples for all directions which we collected to investigate the directional dependence of the fast neutron fluence.

Thermal and epi-thermal neutron fluences can be evaluated using data sets of ^{46}Sc, ^{59}Fe ^{60}Co and so on, which were produced by the (n, γ) reaction with both thermal and epi-thermal neu-

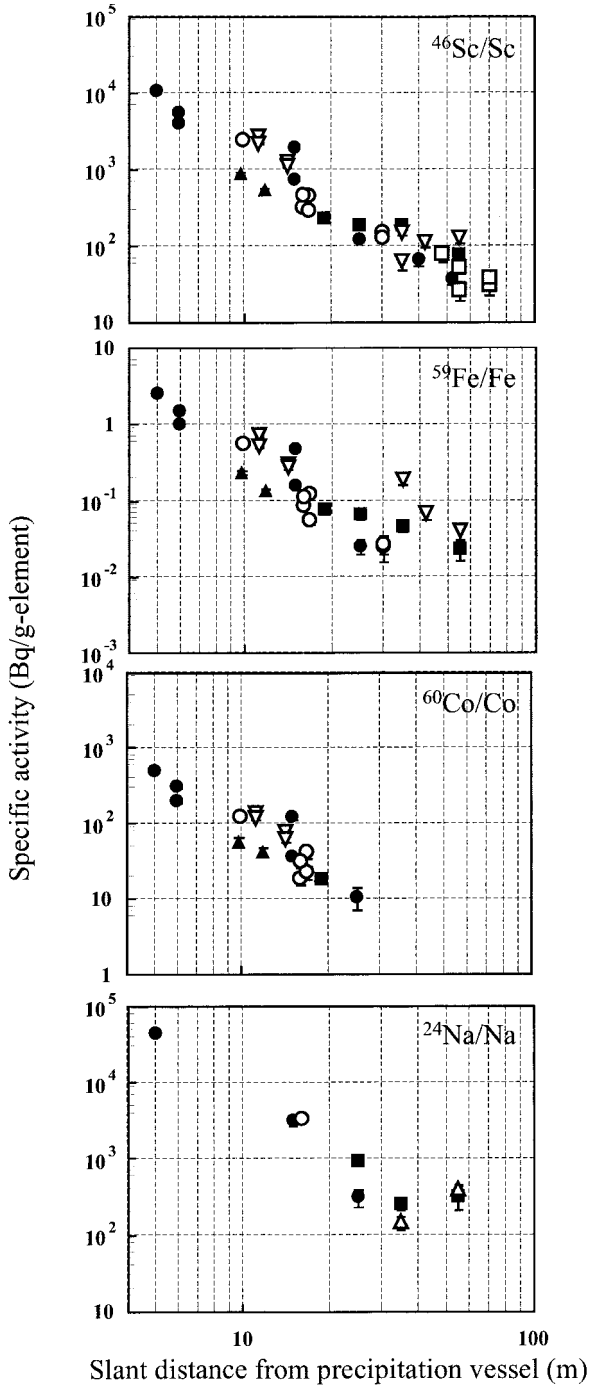

Fig. 5. Plots of specific activities of ^{46}Sc, ^{59}Fe, ^{60}Co and ^{24}Na against the slant distance from precipitation vessel, whose data is separated by 8 directions. ●, NW direction; ▲, NE direction; ■, E direction; ○, SE direction; ▽, S direction and □, SW direction.

trons. The principle of this evaluation method is described by Nakanishi et al.[8]. The method is briefly described below. The specific activity of the induced radionuclide is expressed as

$$A = \lambda N(\phi_{th}\sigma_{th} + \phi_{epi}\sigma_{epi}), \quad (1)$$

where A is the specific activity (Bq/g-element) for the radionuclide of interest, λ is the decay constant (s^{-1}), N is the number of target nuclide per g (g^{-1}), ϕ_{th} and ϕ_{epi} are the thermal and epi-thermal neutron fluences (cm^{-2}) and σ_{th} and σ_{epi} are the neutron capture cross sections for the thermal and epi-thermal neutron reactions, respectively. For the cross section of each target nuclide, the values reported for the well-moderated reactor neutron were used in the calculation for convenience, as listed in Table 3[4]. Binary equations about σ_{th} and σ_{epi} can be derived by substituting the value of the measured specific activity, cross section, decay constant and the number of

Table 3. Cross-section of neutron capture reaction (n, γ) for well-moderated reactor neutron[4].

Nucleus	Cross-section (barn)	
	Thermal neutron	Epi-thermal neutron
^{45}Sc	26.5	13
^{58}Fe	1.15	1.7
^{59}Co	37.2	75.5
^{23}Na	0.53	0.34
^{139}La	9	11.2
^{133}Cs	29	415
^{64}Zn	0.78	1.8
^{121}Sb	4.28	234
^{123}Sb	6.25	127
^{81}Br	2.69	48

target nuclide into the above equation. By plotting such a binary equation for each radionuclide on the same graph, the thermal and epi-thermal fluences can be estimated from the cross-point of the equation lines. However, we must keep in mind that the uncertainty due to the use of cross sections for well-moderated reactor neutrons may cause a disagreement concerning the cross-point. When one cross-point for all lines could not be obtained, the most accordant cross-point was selected by taking into account the cross-point for a set of radionuclides having a larger cross section at thermal neutrons and epi-thermal neutrons, such as ^{46}Sc and ^{134}Cs. When the cross-point did not exist at all, or only ^{46}Sc was detected, the thermal neutron fluence was evaluated by substituting the specific activity of ^{46}Sc into the following equation:

$$\phi_{th} = A / \lambda N\sigma_{th}. \quad (2)$$

Some typical graphs are shown in Fig. 6, and the values obtained for thermal and epi-thermal fluences are listed in Table 4. In the case that cross-point can be obtained from the graph, as

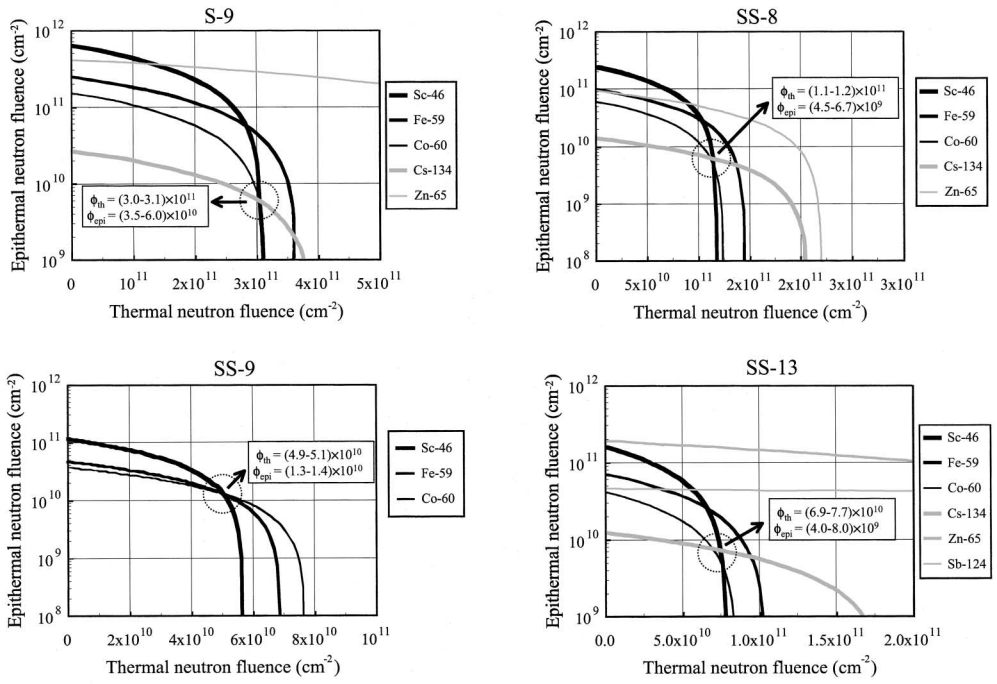

Fig. 6. Estimation of the thermal and epi-thermal neutron fluences.

shown in Fig. 6, the probable range is given in this table, while in the case of equation (2), its value is given with the 1σ error for ^{46}Sc. According to Nakanishi et al.[9], the thermal and epi-thermal fluences of soil sample (S-12) at 10.3m from the precipitation vessel were previously estimated to be 6×10^{10} cm^{-2} and 1×10^{9} cm^{-2}, respectively. Those in the SS-13 soil sample at the same point as S-12 were 7.5×10^{10} cm^{-2} and 7.0×10^{9} cm^{-2}, respectively. The thermal neutron fluence estimated from SS-13 soil agrees approximately with the estimation of Nakanishi et al[9]. Although differences may exist for the epi-thermal neutron fluences, they seem to be rather small.

The fast neutron fluence was also calculated by substituting the specific activity of ^{54}Mn into equation (2). Those in the S-9, SS-7, SS-8 and SS-10 samples were estimated to be 5.6×10^{10}, 5.4×10^{9}, 2.1×10^{10} and 2.9×10^{10} cm^{-2}, respectively. These samples were taken at 5, 10, 6 and 6 m from the precipitation vessel, respectively. The JAERI group[5] estimated the fast neutron fluence to be 6.1×10^{12} cm^{-2}, based on a measurement of the stainless-steel net found 1.8 m from the precipitation vessel. If our data are corrected for the values at 1.8 m with a square of the distance, the fast neutron fluences are expected to be 4.3×10^{11}, 3.0×10^{11}, 2.3×10^{11} and 3.2×10^{11} cm^{-2}, respectively. These estimated values are about 20-times smaller than the value of 6.1×10^{12} cm^{-2}. The disagreement is probably, because the neutron fluence is assumed to decrease simply with the square of distance. The cross section used in the calculation is taken from a well-moderated reactor neutron, which may also cause an underestimation. The ^{54}Mn data must be treated by using the real neutron energy spectrum at each position, which is a future task.

Table 4. Thermal, epi-thermal and fast neutron fluences estimated by surface soil samples.

Sampling points	Neutron fluence (cm^{-2})		
	Thermal neutron	Epi-thermal neutron	Fast neutron
U-5	$(2.2 \pm 0.2) \times 10^{9}$		
U-6	$(5.3 \pm 0.4) \times 10^{9}$		
U-7	$(5.3 \pm 0.2) \times 10^{9}$		
U-8	$(9.2 \pm 0.4) \times 10^{9}$		
S-4	$(3.6 \pm 0.5) \times 10^{9}$		
S-5	$(1.8 \pm 0.4) \times 10^{9}$		
S-7	$(3.5 \pm 0.3) \times 10^{9}$		
S-8	$(2.1 - 2.2) \times 10^{10}$	$(0.4 - 1.0) \times 10^{9}$	
S-9	$(3.0 - 3.1) \times 10^{11}$	$(3.5 - 6.0) \times 10^{10}$	$(5.6 \pm 0.3) \times 10^{10}$
SS-1	$(8.3 \pm 0.6) \times 10^{9}$		
SS-2	$(1.3 \pm 0.1) \times 10^{10}$		
SS-3	$(0.7 - 1.3) \times 10^{10}$	$(2.0 - 6.0) \times 10^{9}$	
SS-4	$(0.5 - 1.0) \times 10^{10}$	$(1.0 - 4.0) \times 10^{9}$	
SS-5	$(1.6 \pm 0.1) \times 10^{10}$		
SS-6	$(2.8 - 3.0) \times 10^{10}$	$(3.0 - 4.0) \times 10^{9}$	
SS-7	$(7.0 \pm 0.2) \times 10^{10}$		$(5.4 \pm 1.4) \times 10^{9}$
SS-8	$(1.1 - 1.2) \times 10^{11}$	$(4.5 - 6.7) \times 10^{9}$	$(2.1 \pm 0.3) \times 10^{10}$
SS-9	$(4.9 - 5.0) \times 10^{10}$	$(1.3 - 1.4) \times 10^{10}$	
SS-10	$(1.6 \pm 0.3) \times 10^{11}$		$(2.9 \pm 0.4) \times 10^{10}$
SS-11	$(1.9 \pm 0.3) \times 10^{9}$		
SS-12	$(1.1 \pm 0.2) \times 10^{9}$		
SS-13*	$(6.9 - 7.7) \times 10^{10}$	$(4.0 - 8.0) \times 10^{9}$	
SS-13	$(6.2 \pm 0.1) \times 10^{10}$		
SS-14*	$(3.1 - 3.3) \times 10^{10}$	$(6.8 - 8.3) \times 10^{9}$	
SS-14	$(3.2 \pm 0.1) \times 10^{10}$		
SS-15	$(4.4 \pm 0.4) \times 10^{9}$		
SS-16	$(3.7 \pm 0.3) \times 10^{9}$		
SS-17	$(4.3 \pm 0.4) \times 10^{9}$		
SS-18	$(3.2 \pm 0.4) \times 10^{9}$		
SS-19	$(2.3 \pm 0.5) \times 10^{9}$		
SS-20	$(1.5 \pm 0.3) \times 10^{9}$		
SS-21	$(1.5 \pm 0.2) \times 10^{9}$		
SS-22	$(7.6 \pm 0.2) \times 10^{9}$		
SS-23	$(8.8 \pm 2.2) \times 10^{8}$		
SS-24	$(1.1 \pm 0.2) \times 10^{9}$		

* These samples were collected by using scoop

1.2 Core soil

The results for the core soil samples are summarized in Table 5. No neutron-induced radionuclides were detected in the SS-23 sample at ca. 70 m from the conversion vessel. Such radionuclides as ^{46}Sc, ^{59}Fe, ^{60}Co, ^{134}Cs, ^{65}Zn, ^{124}Sb and ^{54}Mn were detected in the core samples. ^{46}Sc, ^{59}Fe and ^{60}Co, except for SS-13, were detected even in a deepest layer down to 25cm. ^{54}Mn was observed up to a depth of 15 cm only in SS-8 collected at the nearest point (6 m apart) from

Table 5. Specific activities in core soil samples collected at the second JCO survey.

Sampling points	Depth (cm)	Specific activities (Bq/g–element)						
		^{46}Sc/Sc	^{59}Fe/Fe	^{60}Co/Co	^{134}Cs/Cs	^{65}Zn/Zn	^{124}Sb/Sb	^{54}Mn/Fe
SS-8	0–5	11700 ±200	2.93 ± 0.07	580±20	920 ±230	17 ± 1		0.114 ± 0.007
	5–10	7950 ±140	2.04 ± 0.06	320±10	620 ±130	10 ± 1		0.036 ± 0.006
	10–15	4160 ± 90	0.99 ± 0.03	160±10				0.0091 ± 0.0022
	15–23	1600 ± 40	0.32 ± 0.02	64± 6	110 ± 20			
SS-13	0–5	2530 ± 60	0.55 ± 0.02	110± 8	160 ± 10	7.7 ± 0.7	199 ± 14	
	5–10	1650 ± 50	0.39 ± 0.02	76± 7	110 ± 30	5.9 ± 0.8	78 ± 27	
	10–15	780 ± 30	0.19 ± 0.02	34± 5	69 ± 13			
	15–23	220 ± 20	0.039 ± 0.008					
SS-14	0–5	1140 ± 40	0.087 ± 0.006	41± 4	41 ± 3			
	5–10	1160 ± 50	0.111 ± 0.009	29± 4	0.68 ± 0.13			
	10–15	620 ± 20	0.046 ± 0.004	23± 3	6.1 ± 1.1			
	15–20	390 ± 20	0.038 ± 0.004	23± 4				
	20–25	130 ± 10	0.011 ± 0.004	17± 4				

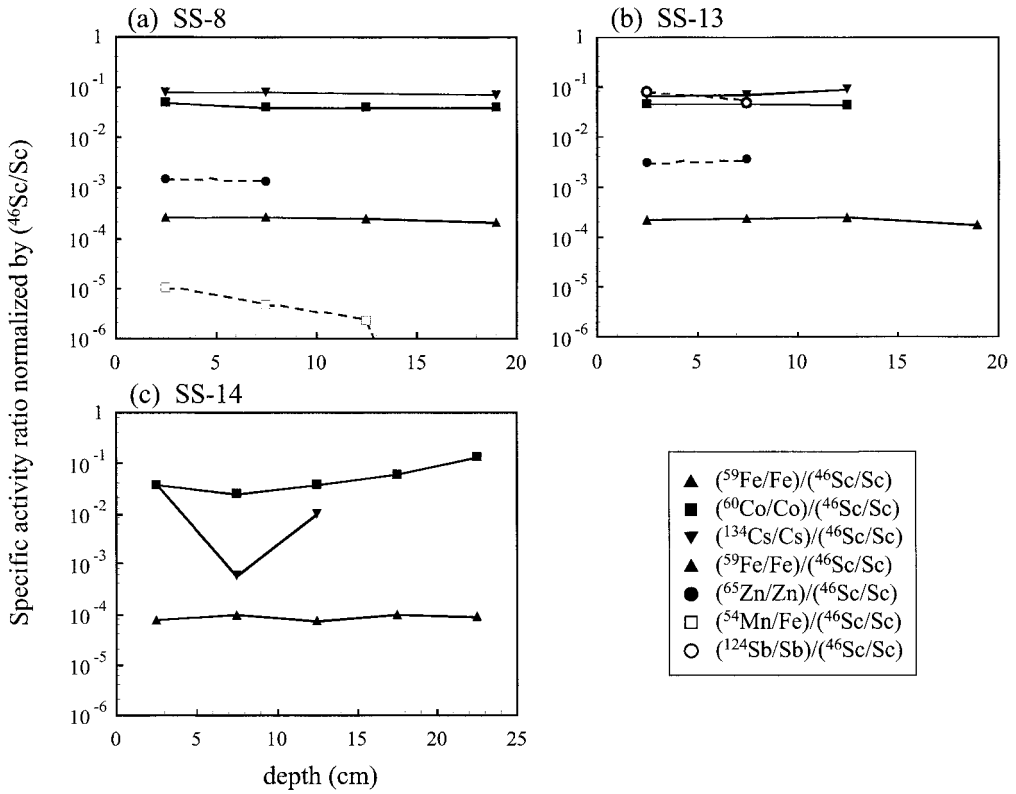

Fig. 7. Specific activity ratios normalized by those of ^{46}Sc in (a) SS-8, (b) SS-13, (c) SS-14 core sample. The ratios of (^{59}Fe/Fe)/(^{46}Sc/Sc), (^{60}Co/Co)/(^{46}Sc/Sc), (^{134}Cs/Cs)/(^{46}Sc/Sc), (^{65}Zn/Zn)/(^{46}Sc/Sc) and (^{124}Sb/Sb)/(^{46}Sc/Sc) were almost constant regardless of the depth , except for ^{134}Cs at SS-14. Only ^{54}Mn decreased with increasing depth.

the precipitation vessel. The specific activities of these radionuclides show the maximum at the top layer, and then decrease monotonically with the depth of soil. ^{45}Sc, which is a target nuclide of ^{46}Sc, has the largest cross section ratio (σ_{th}/σ_{epi}) for thermal to epi-thermal neutrons in all target nuclides in soil. The ratios of the specific activity of each neutron-induced radionuclide relative to that of Sc (e.g. (^{59}Fe/Fe)/(^{46}Sc/Sc)) were used to estimate the contribution of epi-thermal neutrons. These ratios are shown as a function of the depth in Figs. 7(a) - 7(c). Although most of the ratios were constant, only the (^{54}Mn/Fe)/(^{46}Sc/Sc) ratio decreased with the depth in soil. These findings suggest that radionuclides, except for ^{54}Mn, were produced mostly by thermal neutrons. On the other hand, the decrease of the (^{54}Mn/Fe)/(^{46}Sc/Sc) ratio indicates a rapid decrease of the fast neutron fraction due to moderation by moisture contained in soil and soil components.

The estimations of thermal, epi-thermal and fast neutron fluences were also examined using the same method as mentioned above. The results of the analyses are given in Table 6. The epi-thermal neutron fluences were found to be constant independent of the depth. In contrast, the thermal neutron fluences decreased with increasing depth, and were more rapid for fast neutrons.

Table 6. Thermal, epithermal and fast neutron fluences estimated by the core soil samples.

Sampling points	Depth (cm)	Neutron fluence (cm^{-2}) Thermal neutron	Epi-thermal neutron	Fast neutron
SS-8	0–5	$(3.2 – 3.4) \times 10^{11}$	$(1.4 – 2.3) \times 10^{10}$	$(8.5 \pm 0.5) \times 10^{10}$
	5–10	$(2.0 – 2.8) \times 10^{11}$	$(1.0 – 6.0) \times 10^{10}$	$(2.7 \pm 0.4) \times 10^{10}$
	10–15	$(1.2 \pm 0.1) \times 10^{11}$		$(6.8 \pm 0.2) \times 10^{9}$
	15–23	$(4.6 \pm 0.1) \times 10^{10}$		
SS-13	0–5	$(7.2 – 7.5) \times 10^{10}$	$(2.8 – 5.3) \times 10^{9}$	
	5–10	$(4.6 – 4.8) \times 10^{10}$	$(1.3 – 2.4) \times 10^{9}$	
	10–15	$(2.1 – 2.6) \times 10^{10}$	$(1.6 – 5.0) \times 10^{9}$	
	15–23	$(6.4 \pm 0.4) \times 10^{9}$		
SS-14	0–5	$(3.3 \pm 0.1) \times 10^{10}$		
	5–10	$(3.3 \pm 0.1) \times 10^{10}$		
	10–15	$(1.8 \pm 0.1) \times 10^{10}$		
	15–20	$(1.1 \pm 0.1) \times 10^{10}$		
	20–25	$(3.6 \pm 0.4) \times 10^{9}$		

1.3 Concrete block

The specific activities of neutron-induced nuclides in concrete samples are given in Table 7. The concentrations of stable elements were measured only for four samples (COB-1, 6, 8 and 11). For eight other samples, the average value of the four samples was used. The detected radionuclides were ^{46}Sc, ^{59}Fe, ^{60}Co, ^{65}Zn and ^{54}Mn, and to a small extent, ^{152}Eu and ^{154}Eu. As can be seen from this table, the specific activities of radionuclides for the sample COB-8 were the highest among the 12 samples.

Because radionuclides having a larger cross section for epi-thermal neutrons, such as ^{134}Cs, were not detected, the thermal and fast neutron fluences which reached the concrete sample were

Table 7. Specific activities in concrete-block samples (distance: 2.2 m, direction: 270°)*.

Sample number	Specific activities (Bq/g-element)				
	^{46}Sc/Sc	^{59}Fe/Fe	^{60}Co/Co	^{65}Zn/Zn	^{54}Mn/Fe
COB-1	12900 ± 200	4.7 ± 0.4	650 ± 110	3.7 ± 0.3	0.29 ± 0.10
COB-2	13100 ± 100	3.4 ± 0.2	670 ± 50	3.7 ± 0.2	0.12 ± 0.09
COB-3	11500 ± 100	2.0 ± 0.3	580 ± 40	6.7 ± 0.3	0.094 ± 0.044
COB-4	16200 ± 200	3.7 ± 0.7	660 ± 60	5.8 ± 0.3	0.35 ± 0.09
COB-5	17500 ± 200	3.9 ± 0.7	780 ± 70	6.3 ± 0.4	0.11 ± 0.07
COB-6	16700 ± 300	5.5 ± 0.4	760 ± 100	14.0 ± 0.7	0.14 ± 0.13
COB-7	17500 ± 200	4.2 ± 0.6	680 ± 60	6.2 ± 0.3	0.18 ± 0.05
COB-8	21900 ± 300	7.9 ± 0.5	1290 ± 20	6.4 ± 0.5	0.31 ± 0.16
COB-9	20200 ± 300	4.9 ± 0.7	1060 ± 10	16.7 ± 0.6	0.19 ± 0.10
COB-10	15900 ± 200	5.2 ± 0.7	2750 ± 10	4.8 ± 0.3	0.31 ± 0.09
COB-11	17800 ± 300	5.2 ± 0.4	870 ± 120	9.6 ± 0.7	0.28 ± 0.14
COB-12	18200 ± 200	4.3 ± 0.6	900 ± 50	10.8 ± 0.4	0.34 ± 0.08

* See Fig. 2

evaluated in a similar manner as mentioned above (Table 8). The differences in the thermal and fast neutron fluences were found to be a factor of 2 (ranging from 3×10^{11} to 6×10^{11} cm^{-2}) and a factor of 3–4 (ranging from 0.7×10^{11} to 2.6×10^{11} cm^{-2}) respectively. These data may also be compared with the value (6.1×10^{12} cm^{-2} for fast neutron fluence) estimated based on the cross section (2.6×10^{-2} barn) for the ^{54}Fe (n, p) ^{54}Mn reaction in the stainless-steel net sample taken 1.8 m from the precipitation vessel[5]. This concrete block was collected just under the stainless-steel net sample. If the cross section for the stainless-steel net sample can be used for this concrete sample, fast neutron fluence estimated for the concrete sample becomes about three-times larger, and more close to the value from the stainless-steel net.

Table 8. Thermal and fast neutron fluences estimated by concrete-block samples.

Sample number	Neutron fluence (cm^{-2})	
	Thermal neutron	Fast neutron
COB-1	$(3.7 \pm 0.1) \times 10^{11}$	$(2.1 \pm 0.7) \times 10^{11}$
COB-2	$(3.8 \pm 0.1) \times 10^{11}$	$(9.2 \pm 6.6) \times 10^{10}$
COB-3	$(3.3 \pm 0.1) \times 10^{11}$	$(6.9 \pm 3.3) \times 10^{10}$
COB-4	$(4.6 \pm 0.1) \times 10^{11}$	$(2.6 \pm 0.7) \times 10^{11}$
COB-5	$(5.0 \pm 0.1) \times 10^{11}$	$(7.9 \pm 4.9) \times 10^{10}$
COB-6	$(4.8 \pm 0.1) \times 10^{11}$	$(1.0 \pm 0.9) \times 10^{11}$
COB-7	$(5.0 \pm 0.1) \times 10^{11}$	$(1.3 \pm 0.4) \times 10^{11}$
COB-8	$(6.3 \pm 0.1) \times 10^{11}$	$(2.3 \pm 1.2) \times 10^{11}$
COB-9	$(5.8 \pm 0.1) \times 10^{11}$	$(1.4 \pm 0.7) \times 10^{11}$
COB-10	$(4.6 \pm 0.1) \times 10^{11}$	$(2.3 \pm 0.7) \times 10^{11}$
COB-11	$(5.1 \pm 0.1) \times 10^{11}$	$(2.1 \pm 1.0) \times 10^{11}$
COB-12	$(5.2 \pm 0.1) \times 10^{11}$	$(2.6 \pm 0.6) \times 10^{11}$

1.4 Chemical reagents

The specific activities of 9 neutron-induced nuclides found in chemical reagents are listed in Table 9. Among the neutron-induced nuclides measured in the present work, only ^{58}Co is the product by a fast neutron reaction. Although ^{60}Co detected in Raney-Nickel sample was first considered to be produced by the fast neutron reaction ^{60}Ni (n, p) ^{60}Co, the result of NAA showed that ^{60}Co was produced from Co existing as an impurity in Raney-Nickel.

The thermal and epi-thermal neutron fluences which reached the reagent samples of the wet chemistry testing laboratory were evaluated in the same manner as mentioned above. The thermal and epi-thermal neutron fluences were estimated to be $(5 - 5.5) \times 10^8$ cm^{-2} and $(4 - 5) \times 10^7$ cm^{-2}, respectively, from the specific activities for ^{85}Sr, ^{51}Cr and ^{60}Co (Fig. 8). The fast neutron fluence estimated by Raney-Nickel is 2.7×10^7 cm^{-2}. An estimation of the fast neutron fluences was also tried through the measurement of ^{32}P produced by the ^{32}S(n, p)^{32}P and/or ^{35}Cl(n, α)^{32}P reactions in the reagent samples; the following values were obtained: 5.5×10^7 cm^{-2} for an AgCl sample, 1.0×10^7 cm^{-2} for $(NH_4)_2SO_4$ and 2.5×10^7 cm^{-2} for a $BaCl_2$ sample, respectively[10,11]. Considering the above values, the fast neutron fluence at this point lies within the range of $(1 - 5.5) \times 10^7$ cm^{-2}.

Figure 9 summarizes the results of the thermal, epi-thermal and fast neutron fluences estimated from the soil, concrete block and chemical-reagent samples. We believe that these data are useful for estimating the neutron fluences and radiation doses for the residents around the JCO campus. In the future, more accurate neutron fluences at a given point will be estimated by using a neutron-transport model based on the three-dimensional configurations.

Table 9. Specific activities in the chemical reagents at the wet chemistry testing laboratory (distance: 65 m, direction: 80°)*.

Reagents		Specific Activity (Bq/g)
LLRL measurements		
$Sr(NO_3)_2$	^{95}Sr/Sr	$(4.11 \pm 0.31) \times 10^{-3}$
$AgNO_3$	^{110m}Ag/Ag	$(5.92 \pm 0.10) \times 10^{-2}$
$K_2Cr_2O_7$	^{51}Cr/Cr	1.38 ± 0.03
$Ce(NO_3)_3\ 6H_2O$	^{141}Ce/Ce	$(1.60 \pm 0.03) \times 10^{-1}$
Raney-Nickel	^{58}Co/Ni	$(2.15 \pm 0.20) \times 10^{-3}$
	^{60}Co/Co	1.40 ± 0.16
Ogoya measurements		
$Fe(NO_3)_3\ 9H_2O$	^{59}Fe/Fe	$(1.59 \pm 0.17) \times 10^{-2}$
Raney-Nickel	^{58}Co/Ni	$(2.44 \pm 0.14) \times 10^{-3}$
	^{60}Co/Co	0.97 ± 0.69

* See Fig. 2

2. Experiments of neutron-induced radionuclides in soil by a research reactor

For neutron irradiation of a soil sample at UTR-KINKI, the SS-8 soil sample taken 6 m from the precipitation vessel was used. Its results were compared with those of neutron-induced radionuclides in the same soil by the JCO criticality accident. The specific activities of neutron-in-

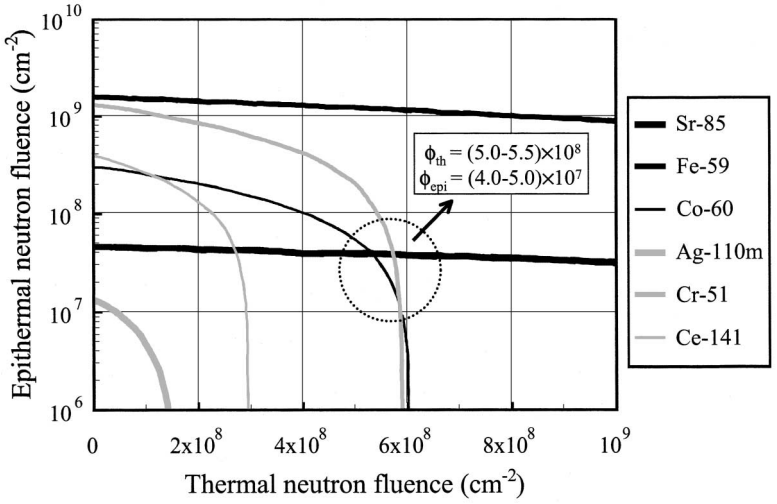

Fig. 8. Estimation of thermal and epi-thermal neutron fluences in chemical reagents. The lines of ^{51}Cr, ^{59}Fe, ^{110m}Ag and ^{141}Ce do not cross each other.

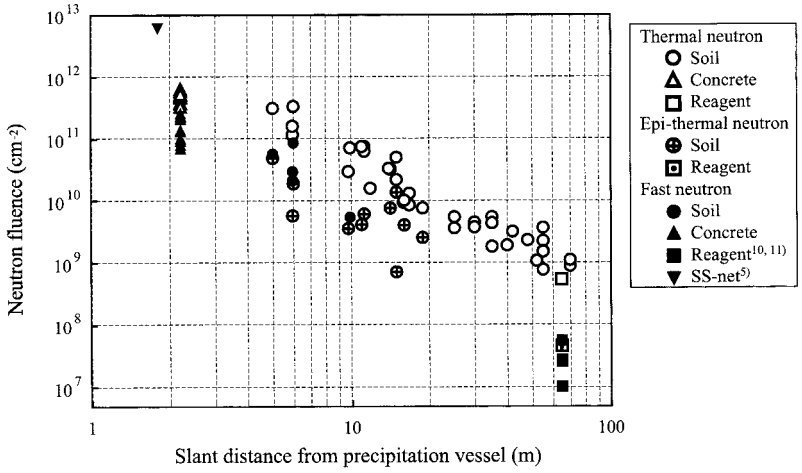

Fig. 9. Plots of the thermal, epi-thermal and fast neutron fluences estimated from the soil, concrete-block and chemical-reagent samples as a function of the slant distance from the precipitation vessel.

duced radionuclides were normalized by the specific activity of ^{46}Sc/Sc to examine the difference in the neutron energy spectrum between the JCO neutrons and the UTR-KINKI neutrons. Their results are given in Table 10. The (^{59}Fe/Fe)/(^{46}Sc/Sc) and (^{60}Co/Co)/(^{46}Sc/Sc) ratios activated by neutrons from the JCO accident agreed well with those by the UTR-KINKI neutrons. In the case of ^{134}Cs, whose target nuclide has a large cross section for an epi-thermal neutron, the JCO value is about 1.2-times larger than that of UTR-KINKI. However, ^{65}Zn from the JCO accident shows a two-times larger value than that of UTR-KINKI, although the ratio of the thermal neutron cross

Table 10. Comparison with specific activities between the SS-8 soil sample activated by leaked neutron at the JCO criticality and by neutron of UTR-KINKI.

	JCO accident (Bq/g-element)	UTR-KINKI (Bq/g-element)
specific activity		
^{46}Sc/Sc	4000 ± 60	4480 ± 70
^{59}Fe/Fe	1.01 ± 0.03	1.15 ± 0.03
^{60}Co/Co	200 ± 10	240 ± 10
^{54}Mn/Fe	0.028 ± 0.004	0.017 ± 0.004
^{134}Cs/Cs	290 ± 30	260 ± 40
^{65}Zn/Zn	25 ± 3	14 ± 2
specific activity ratio		
(^{46}Sc/Sc)/(^{46}Sc/Sc)	1	1
(^{59}Fe/Fe)/(^{46}Sc/Sc)	2.52×10^{-4}	2.56×10^{-4}
(^{60}Co/Co)/(^{46}Sc/Sc)	0.049	0.052
(^{54}Mn/Fe)/(^{46}Sc/Sc)	7.1×10^{-6}	3.9×10^{-6}
(^{134}Cs/Cs)/(^{46}Sc/Sc)	0.073	0.059
(^{65}Zn/Zn)/(^{46}Sc/Sc)	0.0063	0.0031

section to the epi-thermal neutron cross section of ^{64}Zn is smaller than that of ^{133}Cs. From these results, we concluded that the use of the cross sections values for the target nuclides available from the nuclear data may not lead to erroneous results in evaluating the thermal and epi-thermal neutron fluence.

As for the fast neutron, the (^{54}Mn/Fe)/(^{46}Sc/Sc) ratio in the activated sample at the UTR-KINKI was approximately half of that activated by the JCO criticality accident. This indicates that at the point of the SS-8 sample the apparent fast neutron cross section for the ^{54}Fe (n, p) ^{54}Mn reaction was roughly two-times higher than that at UTR-KINKI. Actually, the (^{54}Mn/Fe)/(^{46}Sc/Sc) ratio in SS-8 was 7.1×10^{-6}, which is almost the same as the values of 7.0×10^{-6} in S-9 and 7.0×10^{-6} in SS-10, collected near SS-8. Furthermore, for the SS-7 sample collected at c.a. 10 m from the precipitation vessel, the ratio was found to be 3.0×10^{-6}. The (^{54}Mn/Fe)/(^{46}Sc/Sc) ratio of the concrete samples COB-1, 4, 7 and 10 taken at the top of the concrete sample, were calculated to have similar values of 2.2×10^{-5}, 2.2×10^{-5}, 1.0×10^{-5} and 2.0×10^{-5}, respectively. The concrete sample was located 2.2 m from the precipitation vessel, and nearer than the SS-8 sample. Such a fact that the (^{54}Mn/Fe)/(^{46}Sc/Sc) value decreased with the distance from the precipitation vessel indicate that its value is proportional to the apparent cross section for the ^{54}Fe (n, p) ^{54}Mn reaction. By using equation (3), it is possible to reconstruct the apparent cross section for the ^{54}Fe (n, p) ^{54}Mn reaction at each sampling point at the JCO criticality accident in Tokai-mura, as follows:

$$\sigma_{\mathrm{JCO}} = \frac{(^{54}\mathrm{Mn}/\mathrm{Fe})/(^{46}\mathrm{Sc}/\mathrm{Sc})_{\mathrm{JCO}}}{(^{54}\mathrm{Mn}/\mathrm{Fe})/(^{46}\mathrm{Sc}/\mathrm{Sc})_{\mathrm{UTR}}} \times \sigma_{\mathrm{UTR}}, \tag{3}$$

where σ_{JCO} and σ_{UTR} are the apparent cross section for ^{54}Fe (n, p) ^{54}Mn at the JCO Criticality

Accident and UTR-KINKI, and $(^{54}Mn/Fe)/(^{46}Sc/Sc)_{JCO}$ and $(^{54}Mn/Fe)/(^{46}Sc/Sc)_{UTR}$ are the $(^{54}Mn/Fe)/(^{46}Sc/Sc)$ value at at the JCO criticality accident and UTR-KINKI, respectively. Thus, if the average cross section for the ^{54}Fe (n, p) ^{54}Mn reaction by fast neutrons at UTR-KINKI is evaluated exactly, it may be possible to estimate the fast neutron fluences at each sampling point of the JCO campus.

CONCLUSION

The specific activities of the soil, concrete-block and chemical-reagent samples collected from the JCO campus were measured so as to evaluate the neutrons from the accident. The thermal, epi-thermal and fast neutron fluences were roughly estimated by using the measured specific activities and cross sections for the target nuclides from the nuclear data. The thermal and epi-thermal neutrons decreased as a function of the distance from the conversion building, and their directional distribution was not observed clearly. These data may be useful as basic data in estimating the neutron fluences and radiation doses for the residents. The activation of soil by neutrons at UTR-KINKI provided a possibility for estimating the fast neutron fluence at the JCO campus.

ACKNOWLEDGEMENT

We wish to thank the members of the Atomic Energy Research Institute of Rikkyo University and the University Training and Research Reactor of Kinki University for assistance concerning neutron irradiation. This study was supported by a Grand-in-Aid for Scientific Research from the Ministry of Education, Science, Sports and Culture, Japan (No. 10480024).

REFERENCES

1. "Special Issue on the Tokai-mura Accident" (2000) J. Environ. Radioactivity **50**
2. Murata, Y., Muroyama, T., Kofuji, H., Yamamoto, M. and Komura K. (2000) Neutron-induced radionuclides in soil from the JCO campus by non-destructive γ-ray spectrometry. J. Environ. Radioactivity **50**: 69–76.
3. Muroyama, T., Murata, Y., Kofuji, H., Yamamoto, M. and Komura K. (2000) Neutron activation of chemical reagents released by the JCO criticality accident. J. Environ. Radioactivity **50**: 55–59.
4. Erdtmann, G. (1976) Neutron activation tables. Verlag Chemie; Weinheim.
5. Nuclear Safety Commission (1999) Proceedings of the 66th meeting of the Japanese Nuclear Safety Commission., November 4. STA, Japan, Tokyo. (in Japanese).
6. Takada, J., Suga, S., Kitagawa, K., Ishikawa, M., Takeoka, S., Hoshi, M., Watanabe, H., Ito, A. and Hayakawa, N. (2001) Directional distribution of radiation around an accident at a uranium fuel factory in Tokai-mura, 1999. J. Radiat. Res. **42**: 47–55.
7. Takada, J. and Hoshi, M. (1999) External doses to 350m zone residents around the Tokai-mura criticality accident site. J. Environ. Radioactivity **50**: 43–48.
8. Nakanishi, T., Kobayashi, K., Yamamoto, T. and Miyaji, K. (1987) Residual neutron-induced radioactivities in

sample exposed to the nuclear explosion in Hiroshima. US-Japan Joint Reassessment of Atomic Bomb Radiation Dosimetry in Hiroshima and Nagasaki, Final Report, Vol. 2., pp. 310–319, Radiation Effects Research Foundation, Hiroshima

9. Nakanishi, T., Hosotani, R., Komura, K., Muroyama, T., Kofuji, H., Murata, Y., Kimura, S., Sahoo, S. K., Yonehara, H., Watanabe, Y. and Ban-nai, T. (1999) Residual neutron-induced radionuclides in a soil sample collected in the visinity of the criticality accident site in Tokai-mura, Japan: A Progress Report. J. Environ. Radioactivity **50**: 61–68.
10. Kofuji, H., Komura, K., Yamada, Y. and Yamamto, M. (2000) An estimation of fast neutron flux by ^{35}Cl (n, α)^{32}P reaction. J. Environ. Radioactivity **50**: 49–54.
11. Kofuji, H., Komura, K., Yamada, Y., Sasaki, K. and Yamamoto, M. (2000) An estimation of fast neutron flux from the JCO criticality accident by ^{32}P production rate. Forty-third annual meeting of the Japan Radiation Research Society. 104 (in Japanese)